Renewable and Sustainable Energy Reviews 190 (2024) 114084

Contents lists available at ScienceDirect

Renewable and Sustainable Energy Reviews

journal homepage: www.elsevier.com/locate/rser

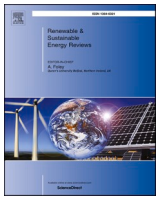

Development of compliant modular floating photovoltaic farm for coastal conditions

Chi Zhang [a], Jian Dai [b,*], Kok Keng Ang [c], Han Vincent Lim [d]

[a] Technology Centre for Offshore and Marine, Singapore, 12 Prince George's Park, 118411, Singapore
[b] Department of Built Environment, Oslo Metropolitan University, 0166, Oslo, Norway
[c] Department of Civil and Environmental Engineering, National University of Singapore, 1 Engineering Drive 2, 117576, Singapore
[d] Building & Research Institute, Housing & Development Board, 310460, Singapore

ARTICLE INFO

Keywords:
Floating PV farm
Photovoltaic
Coastal
Model tests
Energy production

ABSTRACT

Floating photovoltaic (PV) farms can be constructed in coastal marine conditions for the abundant ocean space compared to reservoirs. New challenges may arise when extending existing designs of reservoir floating PV farms to coastal regions because of the complex environmental conditions, especially for the pontoon type floating PV systems. This study presents the methodologies for the design and verification of such floating PV farms based on the practical example of one of the world's largest nearshore floating photovoltaic farms off Woodlands in Singapore. This 5 MW pilot project aims to move floating PV farms from inland water to nearshore regions for future larger-scale deployments. The innovative floating system is adapted from the successful modular floating PV development at Tengeh Reservoir and improved to withstand harsher marine environmental conditions. This study comprehensively introduces various aspects of the development of the nearshore floating modular PV farm, including its design, verification via full-scale experimental testing and numerical studies, construction, and power generation performances. The floating PV system comprises standardized floating modules made of high-density polyethylene (HDPE) that support PV panels or operational and maintenance work. A compliant design allows the floating system to follow wave motion. A verification study was conducted through full-scale experimental tests and numerical simulations based on a representative subsystem of the floating PV farm, focusing on its hydrodynamic performance. Finally, this study presents and discuss the on-site operational energy production performance. This study may serve as a reference for developing large-scale floating PV farms in coastal marine conditions.

1. Introduction

In recent years, renewable energy has become an increasingly important power source worldwide in an effort to reduce carbon emissions. The rapid development of innovative technologies has enabled the capture and storage of renewable energy in a more sustainable and reliable way. Among these technologies, photovoltaic (PV) systems effectively harvest clean solar energy at a low cost. According to the International Energy Agency, solar PV electricity generation increased by a record 18 % in 2021, reaching an impressive 1000 TWh [1].

While PV farms are an effective means of harnessing the solar energy, they require extensive land space to supply sufficient power for fast urban development, which is often unaffordable for land-scarce countries such as Singapore. Despite the extensive placement of PV panels on building rooftops, solar energy cannot meet the fast-growing societal demand for clean and renewable energy [2,3]. As a diverse solution, Singapore has constructed large commercial floating PV farms in inland water bodies after successfully developing a large floating solar testbed in one of its water reservoirs [4]. Similar large floating farms have been constructed in inland water bodies [,5]. This innovative approach has also been adopted in other countries in the region, such as South Korea [6] and Indonesia [7], as well as in other parts of the world [5].

Floating PV farms are more attractive than their onshore counterparts due to their increased efficiency of energy generation, mainly due to the water cooling effect and reduced shadowing from neighbouring buildings and vegetation, and reduced water evaporation of the water body and improved water quality by mitigating the undesirable excessive algal growth thanks to the shielding [4,8–11]. Despite these advantages, limited space remains an issue for Singapore even with full

* Corresponding author.
E-mail address: jiandai@oslomet.no (J. Dai).

https://doi.org/10.1016/j.rser.2023.114084
Received 18 April 2023; Received in revised form 30 October 2023; Accepted 8 November 2023

Nomenclature

Abbreviation

BCS	Buoyancy compensation system
DHI	Danish Hydraulic Institute
DNV	Det Norske Veritas
HDPE	High-density polyethylene
LCOE	Levelized cost of energy
NREL	National Renewable Energy Laboratory
PV	Photovoltaic
RAO	Response amplitude operator
TMY	Typical meteorological year
TRL	Technical readiness level
WKM	Walkway module

Symbols and units

$A(\infty)$	Added mass matrix at the infinite frequency
C_b	Block coefficient (−)
CF	Capacity factor (%)
d	Water depth (m)
D_1	Linear damping coefficient matrix
D_2	Quadratic damping coefficient matrix
E	Average power generation (kWh/m^2/day)
E_{actual}	Actual power generation (kWh)
F^*	Modified Froude number (−)
F_{ext}	External force vector
g	Gravitational acceleration (m/s^2)
H	Wave height (m)
H_s	Significant wave height (m)
K_{res}	Hydrostatic restoring stiffness matrix
L_s	Ship length (m)
L_e	Ship entrance length (m)
M	Structural mass matrix
T	Divergent wave period (s)
T_h	Ship draft (m)
T_p	Wave peak period (s)
U_w	Wind speed (m/s)
U_c	Current speed (m/s)
V_s	Ship forward speed (knot)
W_p	Rated capacity of a PV farm (kW)
α	Hull shape coefficient (−)
β	Empirical coefficient based on ship hull shape (−)
θ	Wave heading (°)

utilization of the water reservoirs. Furthermore, there are concerns about the potential negative environmental impact of floating PV farms on reservoirs, including effects on thermal properties and water circulations [12,13,14].

Unlike onshore land scarcity onshore and sensitive inland water bodies, the ocean space is abundant for developing very large floating PV farms to enable a great amount of solar energy to be harvested. Floating PV farms can be constructed at sea to take full advantage of sun rays, and frequent water circulation minimizes their impact on the marine ecosystem. Several innovative concepts suitable for coastal and offshore conditions have been developed, such as Heliofloat [15], Swimsol [16], SUNdy [17], and a recent concept presented in Ref. [18]. The recent advancements in floating PV farms within marine environments, along with the key challenges and design considerations, have been comprehensively reviewed in Refs. [19,20,21]. To date, however, most concepts and projects on coastal and offshore floating PV farms are at a relatively low technical readiness level (TRL) with a few having been experimentally tested or undergoing test campaigns under marine conditions. Furthermore, the levelized cost of energy (LCOE) of these floating PV farms is found to be high [18], especially for offshore PV farms. Moreover, little has been studied on the power generation performance of such farms in harsh marine conditions.

Compared to calm reservoir conditions, challenging sea conditions with combined environmental actions of wind, waves, and current increase the difficulty of developing floating farms, especially offshore regions. The harsh environmental conditions may significantly increase the cost of construction, operation, and maintenance, and thus the price of generated electricity. In contrast, nearshore coastal waters often provide relatively mild sea conditions with wave heights up to 2–3 m. In Singapore, wave heights can be even smaller than 1 m in sea channels and nearshore regions that are sheltered by islands and other infrastructures [22]. Many novel concepts for nearshore floating structure applications were explored in such conditions [23,24]. The benign sea conditions substantially reduce the design requirements for the supporting floating structures, and are thus extraordinarily attractive for housing large floating PV farms.

While environmental conditions are relatively mild in nearshore water, it is still more complex than inland water reservoir conditions. In a reservoir condition, the design methodology is straightforward, considering only static and human loads as critical load factors. However, in nearshore sea conditions, dynamic loads lead to significant dynamic responses of floating PV farms due to the combined effects of wind, wave, and current actions. The interactions between large floating PV farms and the coastal environment [25] are complex because of the special environmental conditions in coastal waters. These conditions include the prevalence of short waves with small amplitudes, which can excite significant motions of the floater which is of small dimension and lightweight. Also, the passing by vessel can generate significant waves which might superimpose with the nearshore waves [26]. All these factors make it very challenging for the design and verification of large modular floating PV farms under coastal marine conditions.

At the same time, when developing large floating PV farms in the coastal water, one straightforward and economic method is to extend the design of floating PV farms in reservoir conditions to coastal waters. The conventional design of reservoir PV farms comprises large amounts of standardized floating modules to support the PV panels, which as categorized as pontoon-type PV farms by Refs. [20,21]. The floating modules are normally lightweight and of small dimensions for easy fabrication, storage, and transportation. However, the overall dimension of the farm can exceed a hundred meters. In addition, thousands of flexible connectors are often introduced to connect the modules together. These features make it significantly different from the conventional single and multi-body marine and offshore structures, and the experience from the marine and offshore industry may not be directly applicable to the design of floating PV farms. Although DNV recently released the first guideline for designing floating PV farms [27], its provisions are quite general and lack detailed information on how to conduct design in sea conditions.

Concurrently, ongoing research continues to explore this relatively new field, delving into the design methodology and dynamic responses of floating PV farms operating in seawater conditions. Recent advancements in the development of floating PV farms within marine environments, alongside a comprehensive review of the key challenges and design considerations, have been extensively documented [17,25,26]. Analytical solutions developed for the assessment of simplified membrane-type structures have found practical application in the initial design analysis of membrane-type PV farms [28]. Similarly, simulations based on empirical formulas offer an efficient means of estimating the environmental forces to be considered in the design practice [29]. While numerical models relying on computational fluid dynamics can deliver

high-fidelity results for PV farms operating in regular waves [30], their application becomes less cost-effective, especially for large scale floating PV farms under complex environmental conditions. The utilization of potential flow theory, which is widely applied in the analysis of marine and offshore structures [31], has be proven effective for numerical analysis of both rigid and flexible floating PV farms [32–34]. Furthermore, experimental studies have been conducted to investigate small-scale floating PV farms in wave conditions, facilitating conceptual verification and validation of numerical models [35,36]. Such studies can unveil physical behaviours that are not well-known and parameters that are not adequately addressed in the theoretical or numerical studies, thus contributing to the quantification of the associated uncertainties. These experimental studies provide valuable data for the development of PV farms, but they have predominantly focused on idealized environmental conditions. Moreover, in the offshore industry, experimental studies have been primarily conducted on oil production platforms and lately on floating wind turbines, which are often idealized as rigid and single bodies. The experience gained may not be directly applicable to floating PV farms. Very few experimental studies have been conducted for floating PV farms, probably due to the absence of standardized guidance for this type of model testing. One challenge is how to properly model the large floating PV farm in a wave basin. One method is to use a small scaling factor, such as tests in a flume [37] or a towing tank [35]. The challenge in such studies is the scaling effects and the lack of model details. An alternative approach is to propose a representative sub-system and focus on the critical characteristics. This method was successfully implemented in Ref. [22] for a large scale floating hydrocarbon storage facility. Besides, multibody hydrodynamical interactions can become important and should not be simply ignored. The lack of consistent and rational methodology, standardized development, and verification processes for floating PV farms in coastal waters, remains an area of concerns for large-scale project development and realization.

To address these research gaps, this study presents a framework for the development and verification of floating PV farms for use in coastal waters. This framework covers design considerations at the initial design stage, methodologies for design verifications, and evaluation of power generation performance. The successfully launched world's largest coastal floating PV farms in Southeast Asia is used as an example to demonstrate the framework to be presented. Fig. 1 shows the floating PV farm off the coastal of Woodlands, Singapore. It has a peak capacity of 5 MW and comprises 13,312 PV panels, 40 inverters, more than 30,000 floats and a floating barge as converter station. This study encapsulates the whole development procedure of the coastal floating PV farm, including the design considerations, methodology for verifications, and evaluation of operational performance and energy generation.

In this study, the framework for the design, verification and performance evaluation of coastal floating PV farms to be presented addresses several critical aspects that distinguish coastal installations from those in water reservoir conditions. The main original contributions of this study are as follows:

- Coastal-specific design considerations: unique design considerations for coastal water conditions are identified, differentiating them from their counterparts in water reservoirs. These insights were obtained from the development of one of the world's largest coastal floating PV farms.
- Practical design verification methods: this study introduces pioneering design verification techniques that account for coastal wave conditions, including those generated by passing vessels. These methods include numerical simulations considering complex multibody interactions and a cost-effective, scaled laboratory test of a typical subsystem of the entire floating PV farm.
- Real-world power generation performance evaluation: the study presents the site monitoring of the power generation of the floating PV farm. The comparison with numerical models provides valuable data to better understand the actual power generation performance of the deployed floating PV farm.

Although the case study is based on Singaporean coastal conditions, the knowledge gained from this study, especially, the systematic and pragmatic approach can be applied to the design and verification of floating PV farms in coastal waters elsewhere with appropriate modifications and considerations of the site-specific conditions. The findings arising from this study can serve as a valuable reference for further research into coastal and offshore floating PV farms, future development of similar projects, and educated decision-making for policymakers.

The organization of this study is as follows. An overview of the methodology is presented in Section 2. Section 3 presents the design considerations of the PV farm in coastal water conditions, with a focus on the design improvements compared to its predecessor for reservoir conditions. Section 4 presents the consideration of design environmental conditions in nearshore water. Section 5 describes detailed methodologies for verifying the technical feasibility of the floating PV farm design through laboratory model testing, followed by the numerical analysis and comparison in Section 6. The evaluation of the operation and power generation performance of the floating PV farm are presented and discussed in Section 7. The uncertainties of the study are discussed in Section 8. Finally, Section 9 summarizes the major findings arising from this study.

2. Methodology

This section outlines the framework for the design and verification analysis of floating PV farms in coastal marine conditions, while the detailed methodologies for the structural design, design environmental conditions, experimental testing, numerical analysis, as well as power generation evaluation are presented in subsequent sections. Fig. 2 shows the overall framework in this study. Note that the elements in blue color are covered in this study, while those in grey color are considered out of the scope of this work.

The first stage in the design and verification framework is to address critical design considerations for floating PV farms in coastal conditions. These considerations are twofold: structural design and the

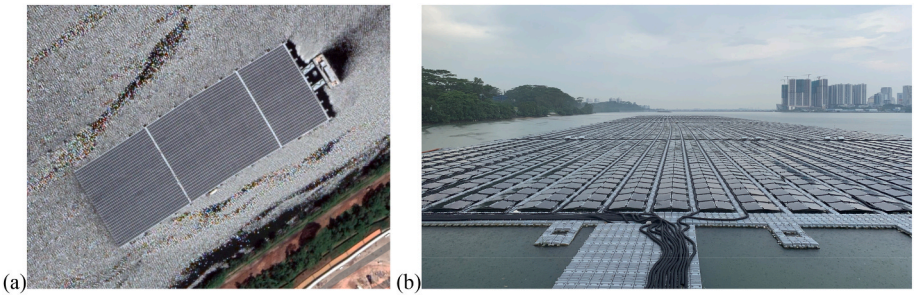

Fig. 1. (a) Satellite view of the 5 MW floating PV farm under construction offshore Woodlands of Singapore; (b) front view of the completed 5 MW floating PV farm.

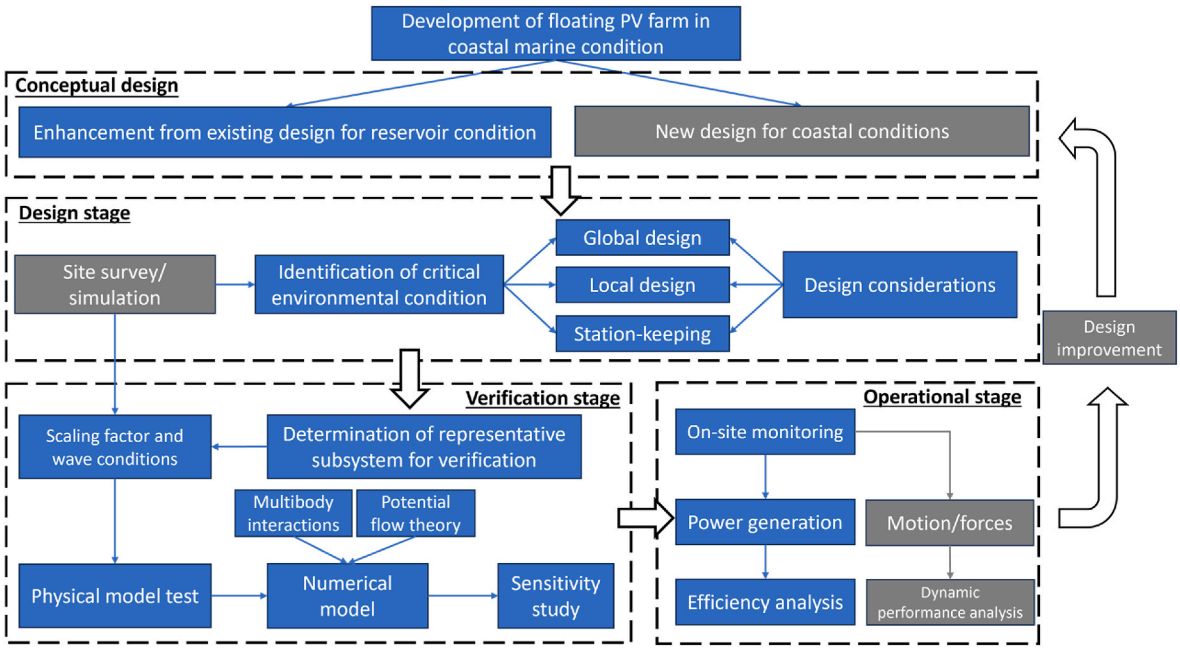

Fig. 2. Flowchart for the framework that covers design and verification of floating PV farms in coastal marine conditions.

determination of design environmental conditions. The structural design contains the development of innovative concepts or improvements to existing farms. It spans both the global and local structural aspects, with a specific focus on implementing a station-keeping system to mitigate horizontal motions. Simultaneously, the determination of design environmental conditions relies on a thorough site investigation and analysis to identify the key factors such as the characteristic wave parameters, water depth, tidal variations, and the frequency of passing vessels. These are drawn from practical experience from the operational floating PV farm in the coastal water of Singapore.

The second stage in the framework is focused on the methodologies for the design verifications. The methodology emphasizes coastal environmental conditions through the combination of experimental testing and numerical simulations. Due to the large footprint of the entire floating PV farm, it is often not affordable to detailly model the entire system. An alternative approach considering a typical subsystem with representative characteristics of the entire farm is proposed for the verification procedure. A full-scale experiment based on Froude-scaling law in a controlled laboratory setting is presented. In parallel, state-of-the-art numerical simulation tools are utilized for analyzing the hydrodynamic performance of the farm under various environmental conditions. A validation of the numerical model through comparison with the experimental data ensures the reliability of the simulation results, especially for such a complex system with a large number of floating bodies considering the multibody interactions, both mechanically and hydrodynamically.

The third stage in the framework involves an evaluation of the power generation performance of the floating PV farm in real-world conditions. Data acquisition systems and monitoring equipment were installed on the farm to collect real-time power yield data. These collected data can be used to study the energy yield and efficiency considering different weather conditions. Furthermore, a post-installation analysis and comparison with the site monitoring data are used to identify the performance ratio and capacity factor of the farm. These can serve as a valuable reference to the future design and projects.

There exist limitations associated with the study. First, the design of the energy systems for the floating PV farms is out of the scope of this work and thus not considered. The design of the energy systems may affect the global configuration of the floating PV farms and thus needs to be considered at an early stage of the development. Second, the design verifications in this study do not encompass the evaluation of aerodynamic loads owing to the fact that the wind speed is rather low in Singapore and the region. For windy areas, the aerodynamic action can result in substantial uplifting forces on the PV panels, affecting the design of the panel-to-floating module and even module-to-module connectors. Third, the power performance analysis does not consider the effect of wave-induced motions of the floating modules on the energy yield from the PV panels. Large motions may influence the power generation performance, but they are not considered in this study due to the benign site wave conditions. Lastly, the actual dynamic responses of the entire floating PV farm are not studied due to the lack of installed structural health monitoring sensors. This limitation is acknowledged for future consideration. Future research is needed to understand the structural and hydrodynamic performances of systems comprising a large number of floating bodies, which can provide important guidance to the design of large scale floating PV farms, floating fish farms, and similar structures.

3. Global and local design considerations

3.1. Global design

The large floating PV farm is a new-generation farm with a modular design and is extended from the design for reservoir conditions as reported in Ref. [33]. The modular design brings in standardized modules to support the PV panel and for operation and maintenance walkways, respectively with semi-rigid connections. The modular design has been proven to be a success in a reservoir condition, which significantly shortens the entire duration of fabrication, construction, and installation. However, to further optimize the modular design and make the farm survive in the sea conditions, a few design improvements have been introduced to this new generation of floating PV farms. Firstly, two basic types of modules were introduced to effectively increase sea space usage, which is important for space-scarce countries. Secondly, high-strength nylon pins instead of stainless steel were used for the inter-modular connection to avoid corrosion. Thirdly, the mooring system has now improved for marine conditions and is capable of handling significant tidal effects in the nearshore water.

The 5 MW nearshore floating PV farm is constructed off the coast of Woodlands in the northern region of Singapore. Fig. 3 shows the global arrangement of the floating PV farm. The farm comprises eight PV zones, each housing 26 by 64 PV panels. The sea space approved for deploying the PV farm is 500 m in length by 100 m in width, while the planar dimension of the floating PV farm is about 447 m by 91 m. This design allows sufficient margins to make sure that the farm will not drift outside the boundaries of the development. For every two pairs of PV panels, there is one lane of longitudinal walkway formed by a single layer of interconnected walkway modules to allow easy access to the panels during maintenance work, as shown in Fig. 4(a). Besides, four 2 m wide walkways formed by two layers of inter-connected walkway modules were introduced as the structural backbone of the farm and a platform for housing combiner boxes and electrical wires. In addition, a floating container is engaged and connected to the floating PV farm which houses the transformer and serves as a monitoring station (see Fig. 4). The power generated by the farm is transmitted through marine cables to the shore from the floating barge.

3.2. Local design

The floating PV farm is mainly formed by connecting two basic types of floating modules, namely the walkway module and the PV module as shown in Fig. 5. Both types of floating modules are rectangular in shape and are made of high-density polyethylene (HDPE). They are modular in design with standard shapes and sizes so that the fabrication and construction costs in mass production are reduced. The walkway modules are designed to carry a load of up to 85 kg due to servicing personnel. The PV floaters are designed to carry a load of 30 kg arising from one PV panel and its accessories. Furthermore, a 15 kg biofouling allowance is considered for both modules considering the local marine growth condition.

To connect different types of floating modules, a special universal connector has been designed, as shown in Fig. 6. The connector includes two major components: T-shape and U-shape at the ends of the floaters that form a shear key for the connector and two standalone vertical nylon bolts which transfer the bending moments developed at the connection. The nylon bolts introduce flexibility to the connectors to allow a limited degree of relative motion freely between the floating modules so that they can move compliantly to the environmental actions. Comprehensive structural tests were conducted to obtain the mechanical properties of the floating modules and the specially designed connections.

The PV panels are connected to the floating modules through a standard back aluminum frame, and the frame is mounted on the floater through embedded nuts. The wind loads acting on the PV panels can therefore be transferred to the floating modules. The detail of the connections between the floating PV module and solar panels is illustrated in Fig. 7. The inclination of the PV panels sitting on the aluminum frame is set to 10°. Note that the theoretical optimal tilt angle in Singapore is almost 0° and the water albedo effect on the power generation of PV panels is rather limited [38]. This 10-degree tile angle is widely adopted as an industrial standard in Singapore to allow rainwater to wash away the accumulated dust and possible bird droppings on the panel surface.

3.3. Station-keeping system

The station-keeping system keeps the entire floating PV farm in place and limits its planar motion within the given boundary. Conventional mooring systems comprising taut mooring ropes and sinkers are found economical and are thus adopted for the nearshore project. However, the design of such a station-keeping system is more challenging when compared to reservoir conditions. Firstly, the water level in the nearshore region varies significantly and frequently due to tidal effects while it varies much less in a water reservoir. The tidal effect can result in up to a 4 m variation in water level according to the site investigation. Considering that the water depth is normally below 20 m for nearshore regions in Singapore, such an effect can lead to a significant change in mooring line tensions and thus the vertical force components acting on tethered floating modules. Secondly, the allowable horizontal motion of the floating PV farm is limited. This leads to a relatively large tension force component needed in the horizontal plane, which will also increase the vertical pull-down forces on the tethered floating modules. If the mooring line tensile forces are large enough and vary significantly, the lightweight floating modules may not have sufficient buoyancy capacity and risk sinking. In other words, the floatation requirement of the floaters may govern the design of the station-keeping system.

To overcome this challenge, a buoyancy compensation system (BCS) is designed and attached to the floating PV farm. The BCS is formed by 10 walkway modules (see Fig. 8), and the mooring ropes are then attached to the BCSs. Each BCS is able to carry a vertical load equivalent to 400 kg. When attached to the floating PV farm, the BCSs carry the vertical mooring load components, leaving only the horizontal mooring load components to the main farm. Such a design significantly increases

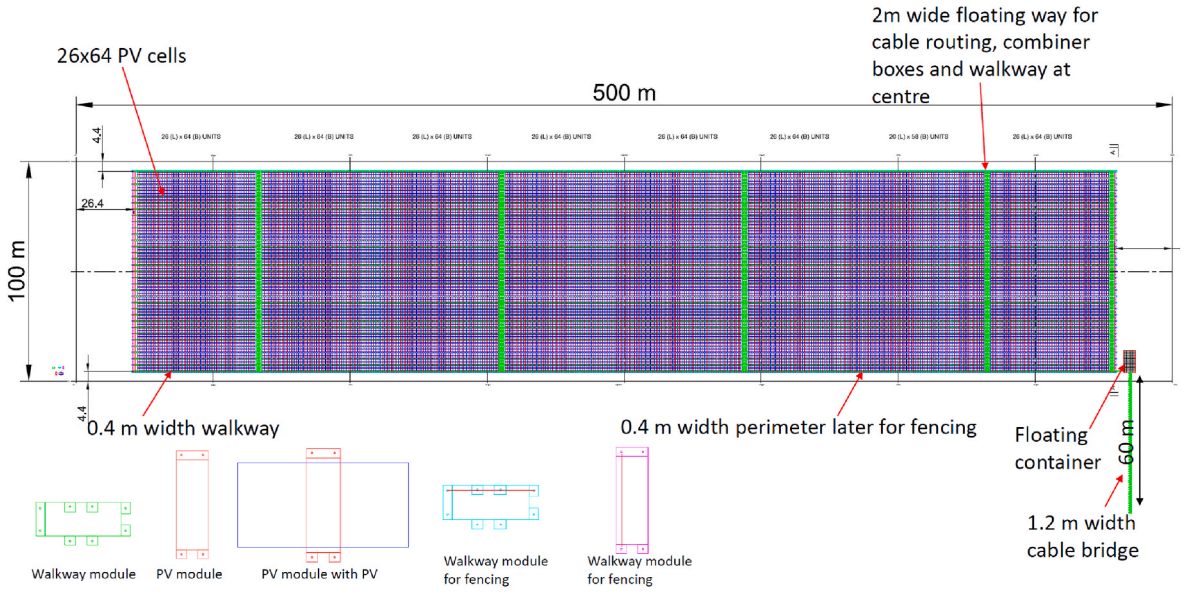

Fig. 3. Floating PV farm: global arrangement.

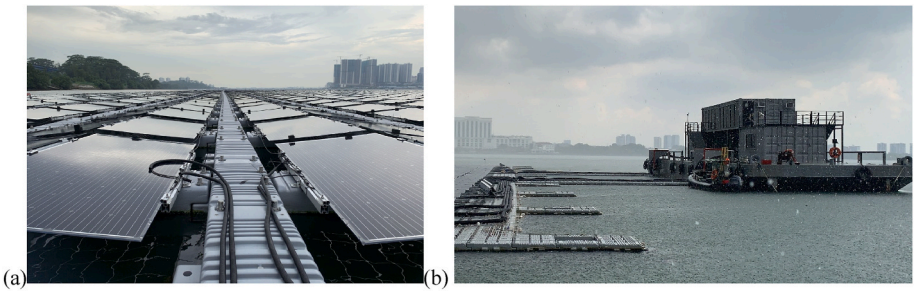

Fig. 4. Floating PV farm off woodlands: (a) walkway modules between PV panels, and (b) floating container housing transformer and control station.

Fig. 5. Walkway module (left) and PV module (right) of the 5 MW floating PV farm.

Fig. 6. Connections between floating modules (left) and nylon bolts for the connectors (right).

flexibility while designing the station-keeping system. It also shows the advantage of the current modular design of the floating PV farm. The final design comprises 52 sets of mooring lines, BCSs, and concrete sinkers (2 tonnes each).

4. Evaluation of environmental conditions

Metocean conditions (wind, wave, and current) are critical for the design of floating PV farms in sea conditions. Apart from the natural metocean conditions such as wind waves, the ship wakes that are generated by passing vessels may significantly influence the dynamic responses of the floating PV farm. Due to limited information available on the passing vessels, an empirical formula is employed to estimate the ship wakes. The ship wakes are assumed to be regular waves and can be linearly superimposed to wind-driven waves.

4.1. Metocean conditions from numerical modeling

The site-specific metocean conditions (wind, wave, and current) at the point of interest off woodlands are were derived from numerical simulations conducted by the Danish Hydraulic Institute (DHI) for the site of the PV farm [39]. The normal and extreme metocean conditions under various return periods for the design and verification studies are defined as follows. The operational condition for the floating PV farm is then defined as the most probable sea states of normal metocean conditions with a return period of 1 year. The extreme condition is defined as storm sea states with a 25-year return period. Because of the limitations in the model test facility, one additional condition is introduced which is defined as the most probable maximum sea condition with a 1-year return period and named as extreme (test). The significant wave height (H_s) and peak period (T_p) of waves, wind speed (U_w), and current speed (U_c) for operational, extreme, and extreme (test) conditions are listed in Table 1. The wave spectrum is assumed to conform to the JONSWAP spectrum given the limited information on the detailed wave properties. It can be seen that the extreme wave condition has quite small wave weights (H_s around 0.2 m). This is due to the fact that the wave conditions around Singapore are generally benign, and this floating PV farm is located in a sheltered channel in the Johor Strait.

4.2. Ship wakes

Ship wakes are a kind of trace generated by a moving vessel on the free water surface, which can be frequently observed in nearshore regions. The pattern of ship wakes is complicated, which includes drawdown, transverse waves and divergent waves. These waves exist around and directly behind the passing ship, and the wave heights and periods depend on the shape of the ships, forward speeds, water depth under keel clearance, etc. The divergent waves, which are also known as sec-

Fig. 7. Details of PV panel supporting frame mounted on the PV modules (unit: mm).

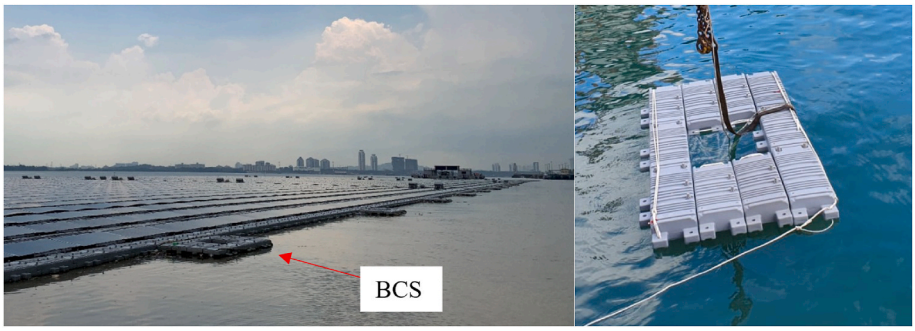

Fig. 8. Buoyancy compensation system installed for floating PV farm off Woodlands, Singapore.

Table 1
Operational, extreme (test) and extreme environmental conditions.

Sea condition	H_s (m)	T_p (s)	U_c (m/s)	U_w (m/s)
Operational	0.03	1.0	0.01	2.2
Extreme (test)	0.1	1.7	0.01	2.2
Extreme	0.2	1.7	0.05	13.6

ondary waves are of the main interest in this study because they can propagate to the floating PV farm and influence its dynamic responses. Although ship wakes can be simulated through proper numerical techniques [40,41], the limited available information and substantial computational resources often constrain and may even prohibit their applicability for practitioners. Alternatively, a few practical formulas have been developed and can be employed as an efficient method to estimate the wave height of ship wakes, especially for divergent waves. An empirical formula derived by Kriebel and Seelig [42] is adopted in this study to quantify wake height H induced by vessels sailing around the floating PV farm.

$$H = \beta \frac{V_s^2}{g}(F^* - 0.1)^2 \left(\frac{y}{L_s}\right)^{-\frac{1}{3}} \tag{1}$$

where β is the empirical coefficient based on ship hull shape, V_s is ship forward speed, g is gravity acceleration, y is the distance of the point of interest from the sailing line, L_s is the ship length, and F^* is modified Froude number. β and F^* can be determined by the following formula:

$$\beta = 1 + 8\tanh^3\left(0.45\left(\frac{L_s}{L_e} - 2\right)\right) \tag{2}$$

$$F^* = \frac{V_s}{\sqrt{gL_s}} \exp\left(\alpha \frac{T_h}{d}\right) \tag{3}$$

where L_e is the ship's entrance length and equals the distance from the bow to the start of the parallel mid-body, T_h and d are the ship draft and water depth, respectively, and $\alpha = 2.35(1 - C_b)$ is the hull shape

coefficient, with C_b the block coefficient.

The period of divergent waves can be estimated from the velocity of the vessels [43] as

$$T = 2\pi V_s \frac{\cos\theta}{g} \tag{4}$$

where θ is the angle of wave propagation. Here, the deep-water assumption is assumed valid in this study for the divergent waves, and the theoretical value of θ equals 35.3° under this assumption.

It should be noted that the vessels that sail around the sailing line close to the floating PV farm are normally tugs and barges. Due to the lack of detailed information, a typical tug sailing around Singapore is selected for the ship wake analysis. Note that the water depth is assumed to be uniform at 15 m, and the distance of the vessel from the edge of the floating PV farm is taken as 20 m. The speed of the tug is assumed to be 6 knots in operational conditions. The key parameters of the tug and the corresponding wave height and period of the secondary waves are listed in Table 2. It can be seen that the ship wakes have a similar magnitude to the extreme wind waves as shown in Table 1. This shows the importance of considering ship wakes in the analysis of the floating PV farm in the nearshore region.

5. Design verification: laboratory tests

Careful verification of the floating PV farm design should be carried out to ensure safe operations. The entire farm is based on a basic cluster of the floating PV farm comprising 10 connected modules, which is treated as a typical subsystem of the floating PV farm.

To ensure that the hydrodynamic performance of the floating modules and the structural capacity of the connections are satisfactory as designed, detailed laboratory tests on a subsystem of the floating PV farm were conducted. The rationale behind this is that the wavelength in the nearshore region is short, and the wave-frequency motion of floating modules or the local responses of the floating PV farm is more important than the global responses. This can also be supported by the results of the hydroelastic analysis reported in Ref. [22] where the deformation of the floating PV farm is dominated by local responses of the floating modules. The subsystem under testing is shown in Fig. 9. The key parameters are summarized in Table 3. In addition to verifying the hydrodynamic performance, the model test also serves as an important benchmark to verify the numerical models that enable more detailed case studies to be conducted numerically. Note that the ship wakes, wind, and current were not considered in the model test. Instead, they will be considered in the parametric studies using verified numerical models.

5.1. Hydrodynamic model tests

The model tests on the subsystem were performed in the coastal wave basin, hydraulic laboratory, National University of Singapore. The wave basin has an overall dimension of 24 m × 10 m × 0.9 m (length by width by depth). The basin permits a maximum water depth of 0.75 m. The basin is equipped with 13-unit piston-type wave paddles on one end. It can generate waves with periods from 0.5 to 3.5 s and with a maximum wave height from 0.05 to 0.3 m with a 0.6 m water depth. At another end of the basin opposite the wave paddles, a passive gravel beach is set to absorb the wave energy to reduce the reflection rate in the basin to around 10 % (amplitude) of the incident waves. Considering the condition of the wave basin, the subsystem was tested on the full scale. Both regular wave and irregular wave tests were conducted. Due to the constraint of the wave generation system, the incident waves were carefully chosen, and the wave parameters and the test matrix are listed in Table 4. The water depth was set to 0.45 m, and only head sea conditions were considered. Each run of the model tests lasted for 100 s for regular wave conditions and 700 s for irregular wave conditions. The incident waves were calibrated before the model test through wave gauges placed at the location of the subsystem.

Table 2
Key parameters of a tug operating around Singapore and the wave parameters of the ship wakes.

Key parameters	Values
L_s (m)	32
B (m)	10
T_h (m)	5
C_b	0.65
L_e (m)	8
y (m)	20
V_s (knot)	6
T (s)	1.62
H (m)	0.126

The model test setup is shown in Fig. 9. The subsystem of the floating PV farm was placed in the centre of the wave basin, and the front edge of the subsystem was 7.4 m away from the wavemaker. Six walkway modules and four PV floater modules were connected the same way as in the prototype. Solid ballast was placed on top of the PV module to represent the weight of the PV panels and their accessories. The subsystem was connected to an aluminum frame which was mounted on the carriage through hinge connectors. During the model test, the focus was placed on the motion of the modules. The 6°-of-freedom motions of two walkway modules (see Fig. 9 (a)) were measured through the Phase-Space motion tracking system. In addition, the wave heights in front of and between the two layers of PV floaters were recorded during the model test. The sampling rate for motion tracking was 60 Hz, while it was 50 Hz for wave elevations. Both signals were resampled to 25 Hz during the data post-processing.

Note that two coordinate systems are introduced to describe the motions of the floating modules. One is the body-fixed coordinate system. The origin of a body-fixed coordinate system locates at the centre of each floater's water plane. The x-axis points towards the wave paddles, and the z-axis points upwards from the water plane. The y-axis can be determined through the right-hand rule. Another is the global coordinate system $OXYZ$ whose origin locates at the geometrical centre of the water plane of the entire subsystem, and the definitions of X, Y and Z axis are the same as the body-fixed system.

5.2. Model test results

From the recorded motions of the floating modules, the motion response amplitude operators (RAOs) can be derived. An advanced technique termed the focused white noise test was utilized. The tests generate focused wide-band wave groups to derive the RAOs of the floating modules in a short duration. This method was introduced for the model test of a floating oil large floating structures in nearshore water and has been proven to give promising results and minimize the effect of wave reflections in small-scale wave basins [21].

The motion RAOs of the first and second walkway modules (WKM 1 and WKM 2) in heave and pitch degrees of freedom in head sea conditions are shown in Fig. 10. In these figures, the unit is set to centimetres. Note that only linear parts of the waves and responses are kept for deriving the motion RAOs of the floating walkway module. It can be found that the motion RAOs obtained from the regular waves show a good agreement with those obtained from focused white noise. For short waves with periods smaller than 0.7 s, both the heave and pitch motions of the floating modules are found to be quite small. Such short waves cannot excite significant motions of the floating modules. However, for wave periods around 1 s where the wavelength is close to the module's length, the heave RAOs show a significant peak. By comparing the motion RAOs between the two walkway modules, the difference in heave is significant for wave periods between 0.8 and 2.5 s while the difference in pitch is rather small for all wave periods tested. It is also

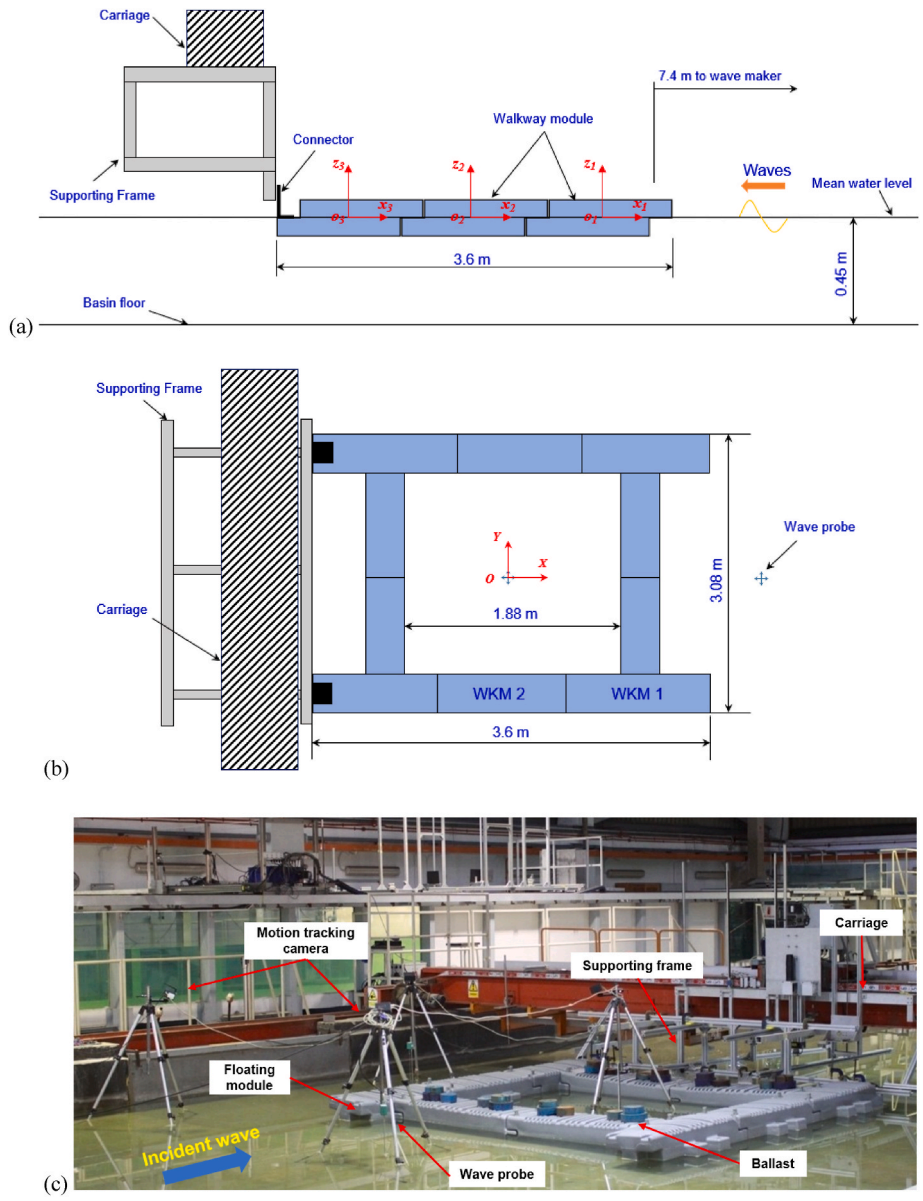

Fig. 9. Floating PV farm: global arrangement, and mooring distributions.

Table 3
Key parameters of a subsection of the floating PV farm for laboratory test.

Key parameters	Values
Overall length (m)	32
Overall width (m)	10
Draft at front edge (m)	5
Displacement (kg)	0.65
Self-weight (kg)	17.2
Ballast weight (kg)	160

Table 4
Hydrodynamic model test matrix for the subsystem of the floating PV farm.

Wave type	Wave height (H or H_s)	Wave period (T or T_p)
Regular waves	0.03	0.6–1.3 (0.1s interval)
Irregular waves (operational)	0.03	1.0
Irregular waves (extreme, test)	0.10	1.7
Focussed waves (wide band)	0.05	0.3–3.0

observed that the global motion of the subsystem is dominating within this wave frequency range. This will be further discussed in Section 5.

The dynamic responses of the two floating walkway modules subjected to the random waves (operation and extreme conditions) were also measured. The response spectra in the heave and pitch degrees of freedom of the two floating walkway modules (WKM 1 and WKM 2) under the operational and extreme sea conditions are shown in Fig. 11. In general, the external floating walkway module exhibits the largest responses, especially in the heave direction. The responses are almost negligible under the operational condition when compared to the extreme condition. These observations are consistent with those observed in Fig. 9. For long waves under the extreme sea condition, the response spectrum tends to be narrower banded in contrast to the operation condition. This may be explained by the fact that the entire structure tends to move as one rigid body under long waves and the effect of hydrodynamic interactions and mechanical couplings between the different modules are much reduced as compared to that under the operational condition.

The statistics of the motion responses of the floating walkway module in the operational condition and extreme condition are shown in

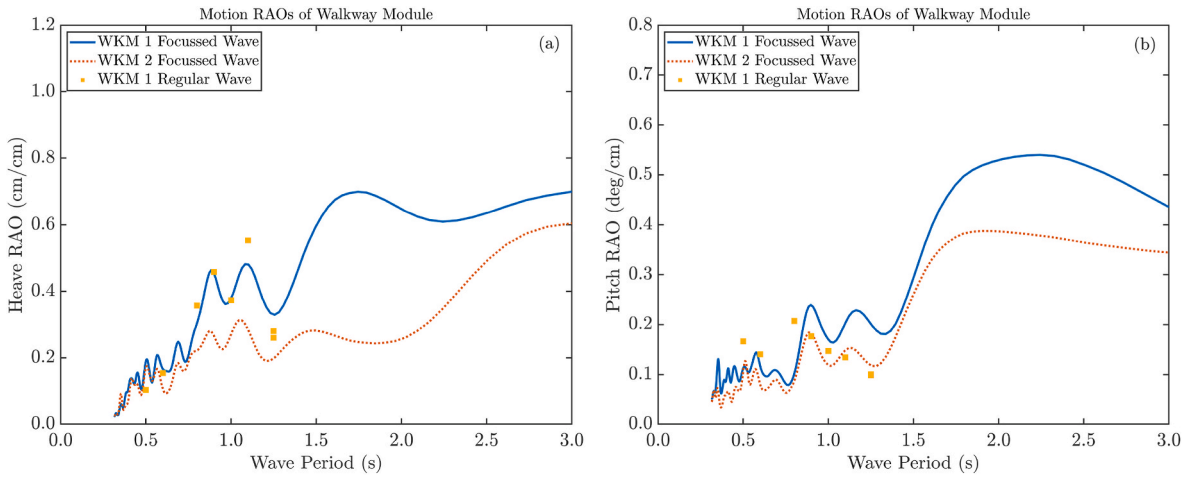

Fig. 10. Motion RAOs of floating walkway modules in (a) heave and (b) pitch.

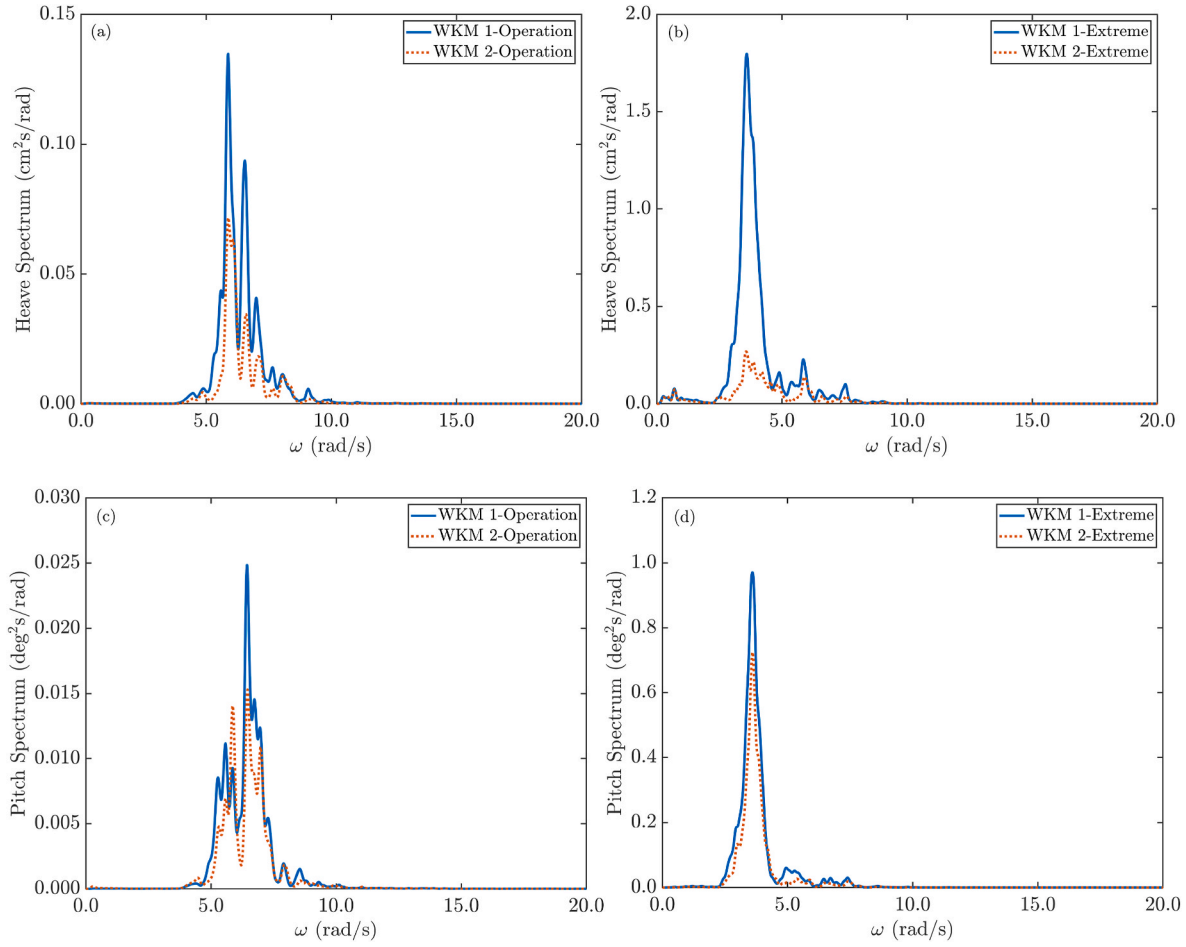

Fig. 11. Motion response spectra in heave and pitch for walkway modules in (a) & (c) operational and (b) & (d) extreme conditions.

Figs. 12 and 13, respectively. It can be seen that the maximum heave motion in the operational condition is smaller than 1.5 cm, while in the extreme condition, the maximum heave can be up to around 5 cm. Both are significantly smaller than the draft of the floating walkway module which is 12 cm. The pitch motion of the outermost module under the extreme condition is smaller than 4 deg. All these results suggest that the motion responses of the floating modules are at an acceptable level. It is also observed that the motions of the second floating walkway module (WKM 2), as expected, are generally smaller than those of the first walkway module (WKM 1). The results support that the motions of the outermost floating modules are prone to larger motion responses. Such an observation is consistent with the previous studies conducted by the authors on modular floating structures [24,44]. Consequently, the exterior floating modules, especially those facing the weather side, should be given extra attention in the design and maintenance checks of the floating PV farm.

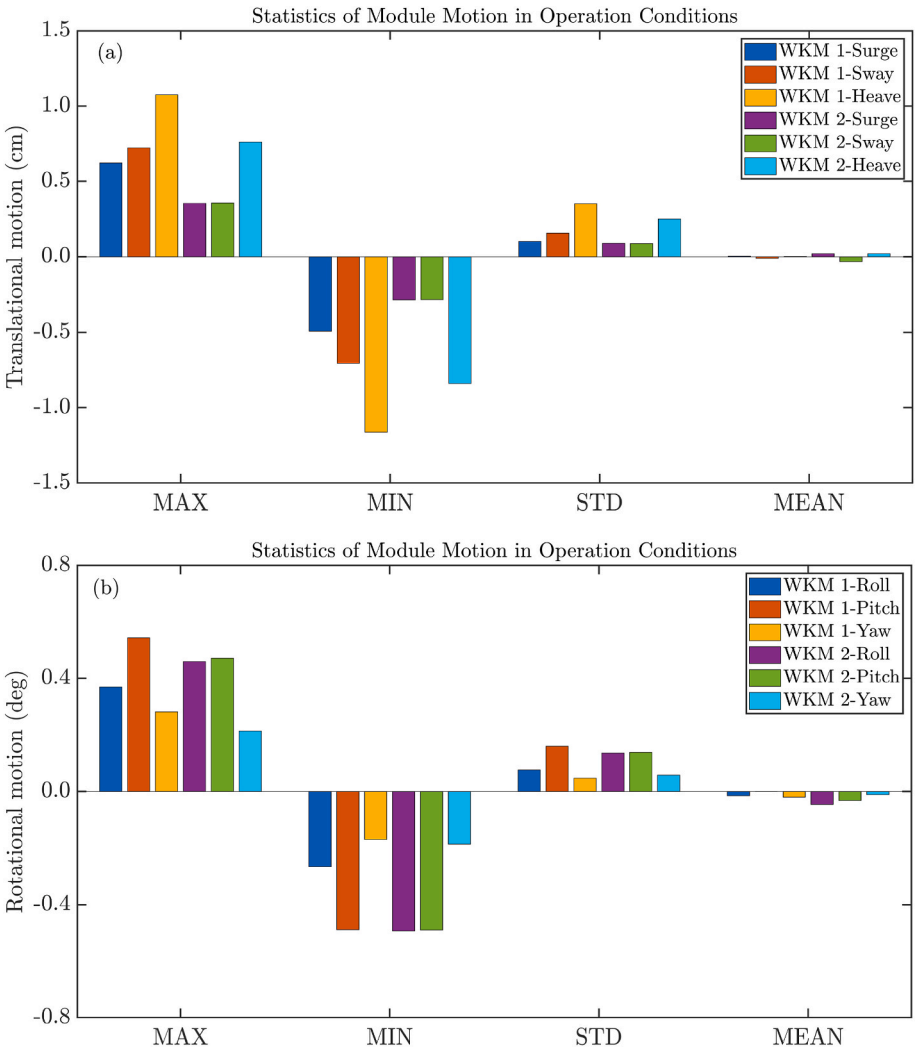

Fig. 12. Statistics of (a) translational motion and (b) rotational motion of floating walkway modules in operation condition.

6. Design verification: numerical analysis and comparisons

To further examine the dynamic performance of the selected subsystem of the floating PV farm, a time-domain numerical model which is based on potential flow theory was established. In view of the fact that the floating modules are of pontoon type, direct numerical modeling of the hydrodynamic actions on the floating system is selected among a few numerical methods as reviewed in Ref. [18]. Due to the existence of nonlinearities in the model tests and prototypes, for example, the viscous effects from waves, drag forces from current, and the nonlinearities from mooring lines and fenders, a time-domain analysis is preferred. To account for these effects, a hybrid frequency- and time-domain method based on the equation proposed by Cummins [45] is adopted. This method transfers the linear frequency-domain hydrodynamic coefficients into the time domain, and the equations of motion for a single rigid floating body can be written as:

$$(M + A(\infty))\ddot{x}(t) + D_1\dot{x}(t) + D_2\dot{x}(t)|\dot{x}(t)| + \int_0^t h(t-\tau)\dot{x}(\tau)d\tau + K_{res}x(t) = F_{ext}(t, x, \dot{x}) \quad (5)$$

where M and $A(\infty)$ are the structural mass matrix and the added mass matrix at the infinite frequency, respectively; $x(t)$, $\dot{x}(t)$, $\ddot{x}(t)$ are the displacement, velocity and acceleration vectors in the time domain, respectively; D_1 is the linear damping coefficients matrix, D_2 is the quadratic damping coefficient matrix which represents the viscous effect for pitch and roll direction; K_{res} is the restoring matrix due to hydrostatic forces; $F_{ext}(t, x, \dot{x})$ is the summation of all external forces in the time domain, and it includes the first-order and low-frequency wave excitations, current and wind forces, and mooring forces, etc. The low-frequency wave excitation force is approximated by Newman's approximation. The hydrodynamic coefficients, namely, the added mass, potential damping, and wave excitation forces can be calculated from commercial or open-source boundary element method based codes, such as WAMIT [46] and NEMOH [47]. In this study, NEMOH is used to calculate these coefficients. The time-domain simulations are conducted by using the Open-source code WEC-Sim [48].

The numerical model of the subsystem is shown in Fig. 14. The hydrodynamic interactions between the floating modules are considered in

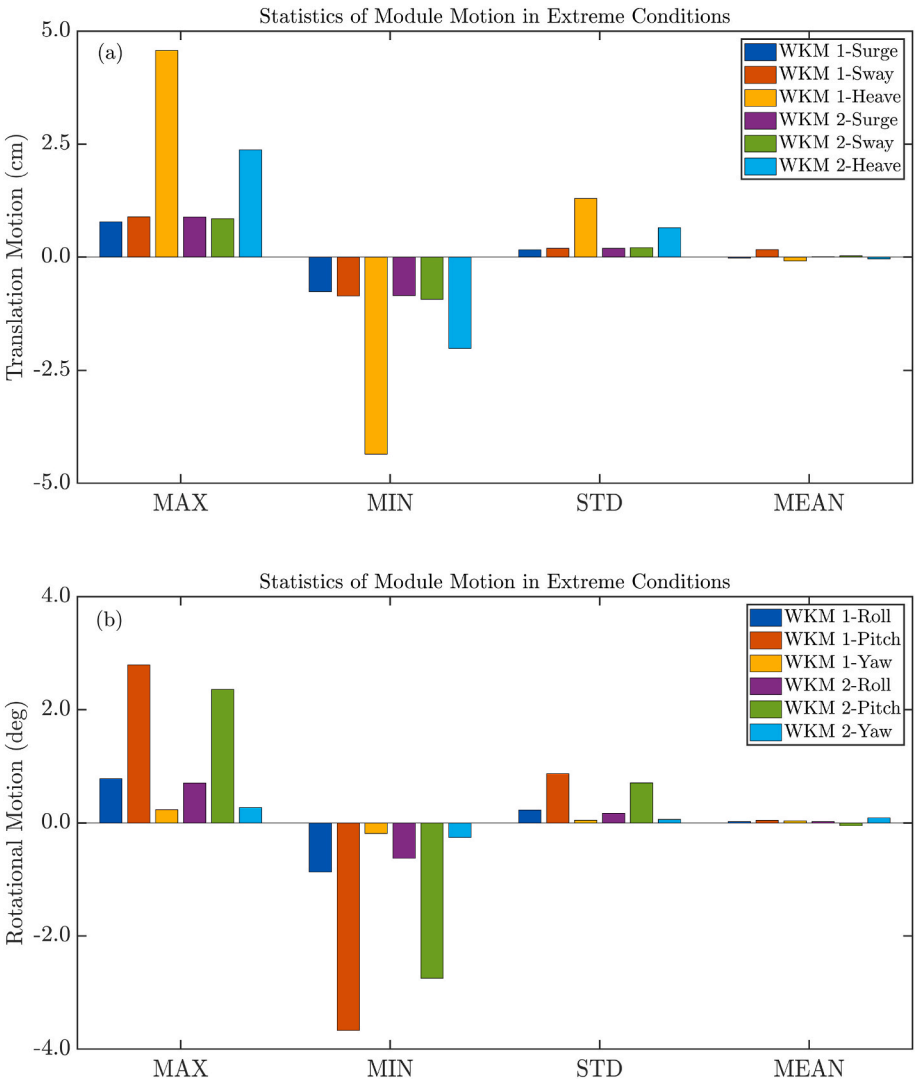

Fig. 13. Statistics of (a) translational motion and (b) rotational motion of floating walkway modules in extreme conditions.

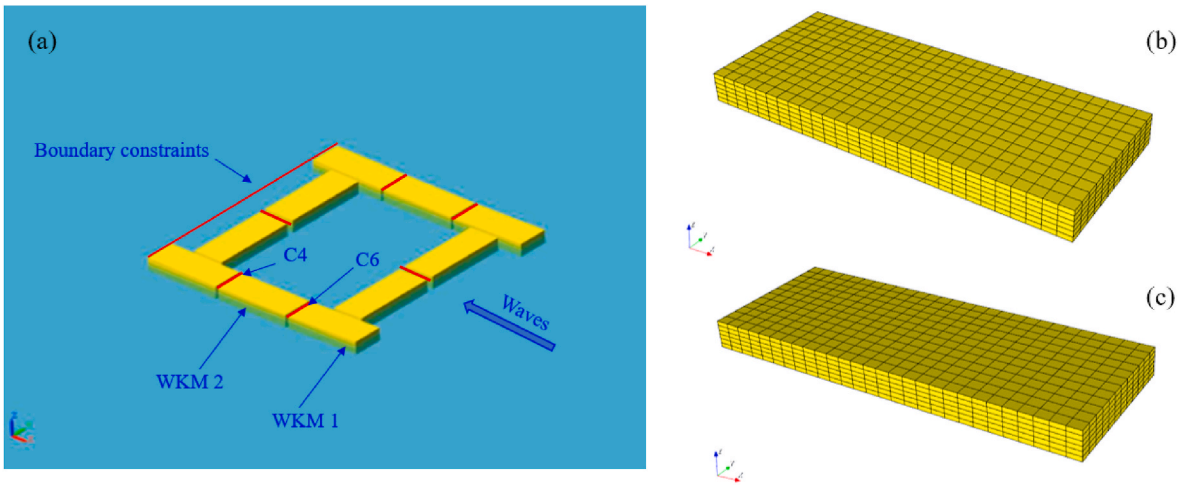

Fig. 14. Numerical models of the subsystem of the floating PV farm: (a) time-domain model, (b) mesh of the walkway module, and (c) mesh of the PV module.

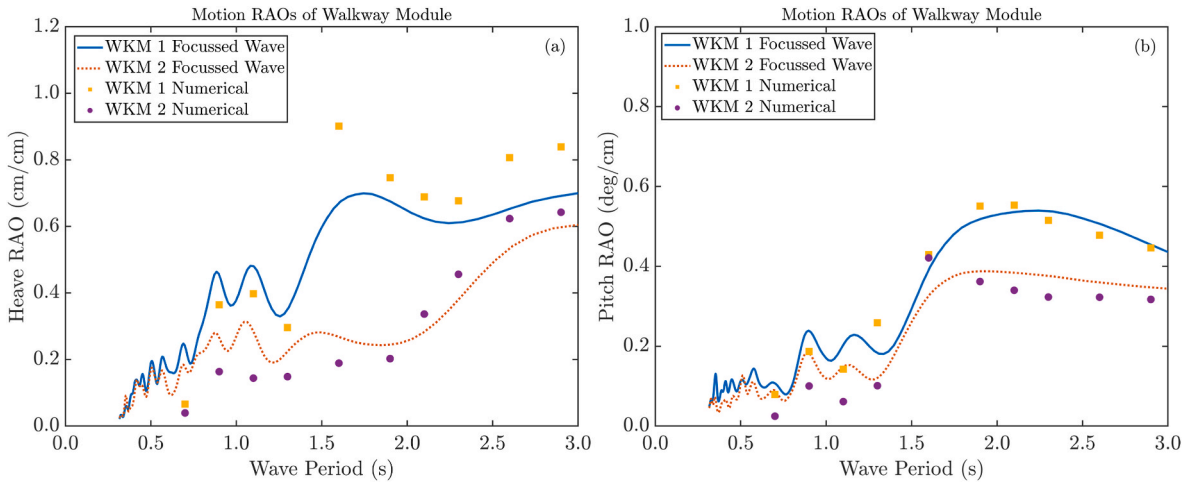

Fig. 15. Comparison of motion RAOs from numerical model and model tests in (a) heave and (b) pitch.

the frequency domain analysis and are thereafter transferred into the time domain model. The constraints in the model are considered as flexible joints with stiffness derived from the structural tests [33]. The floating modules are assumed to be rigid bodies in the simulation. The duration of each simulation is set to be the same as that in the model tests. For random wave conditions, the calibrated incident waves from the model tests are used as the input for the numerical simulation. The effect of ship wakes is considered by adopting the linear superposition method.

Uncertainties in the simulation and model tests include the frictional forces from the connections, viscous damping for every single model, and the misalignment during the model installation. These uncertainties will be further justified in the analysis of a harsher sea state.

6.1. Validation of numerical models

Fig. 15 shows the comparison of the motion RAOs of two walkway modules in heave and pitch between the numerical and model test results. A fairly good agreement can be found between the two models, especially for the RAOs under long wave excitations. Some discrepancies can be found when the waves are short, and these could be attributed to the uncertainties in the model tests when the motion responses are very small. Fig. 16 shows the motion response spectrum for the two walkway modules from the numerical model and model tests. Again, the comparison shows that the numerical model can well capture the dynamic responses of the subsystem of the floating PV farm. It is noticed that the numerical model tends to overestimate the heave responses. This may be because the additional damping due to the viscous effect in the heave direction is not included in the current numerical model.

6.2. Response in actual extreme waves

Based on the validated numerical model, the simulation is further extended in this study for more complex and realistic scenarios. The first scenario considers the actual extreme sea condition (see Table 1), while the second scenario superposes the actual extreme sea condition with a regular wave generated by a passing vessel to investigate the effect of ship wakes. In the third scenario, mooring lines are added to connect the outermost modules in the numerical model, reflecting the actual prototype design. In the numerical model, the mooring line stiffness is linearized to 1840 N/m. This scenario intends to identify the effect of mooring lines on the outermost modules. Fig. 17(a) and (b) show the heave and pitch response spectra of one outermost walkway module (WKW 1, see Fig. 14) under different scenarios. Note that the extreme sea conditions considered in the experimental model test (see Table 4) are also employed for the purpose of comparison. It can be found that the actual extreme environmental conditions can lead to much higher motion responses of the floating modules in both heave and pitch. Ship wakes induce narrow-band sharp response spectra, which is expected to increase the motion responses. By introducing the mooring lines, both the heave and pitch motions of the outermost module can be reduced, and the reduction in the pitch motion is observed to be more significant.

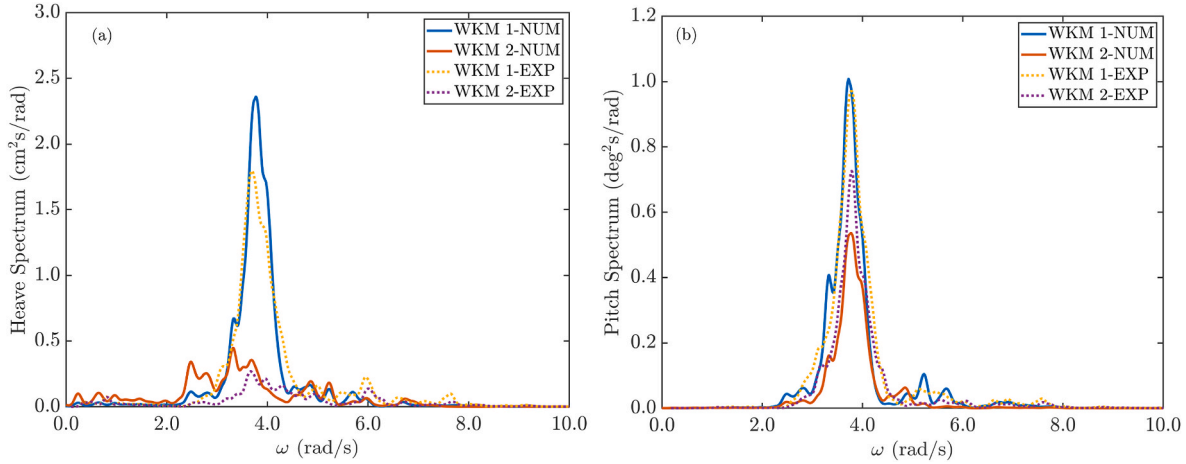

Fig. 16. Comparison between numerical and experimental motion response spectrum in experimental extreme sea conditions for (a) heave and (b) pitch.

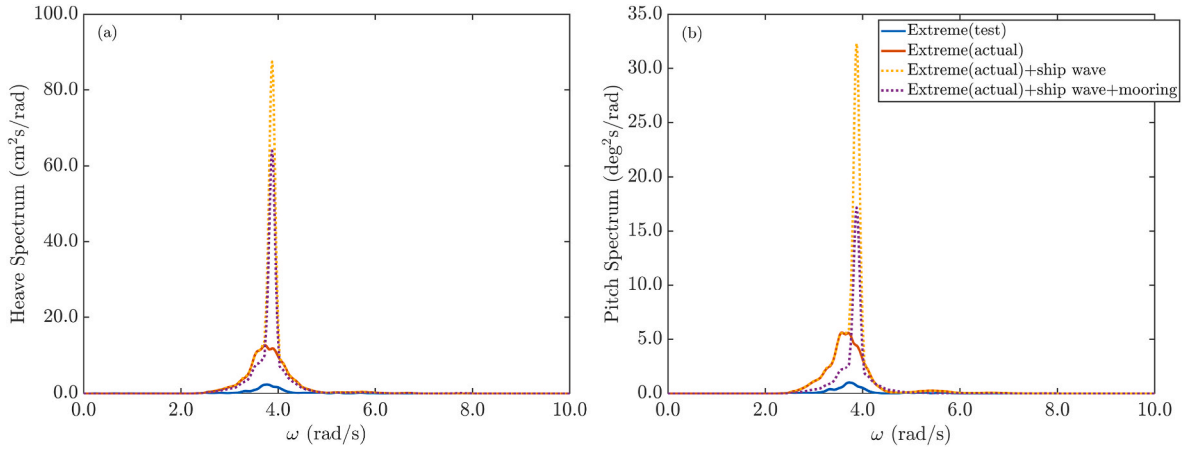

Fig. 17. Comparison between numerical and experimental results: motion response spectra in actual extreme sea conditions for (a) heave and (b) pitch.

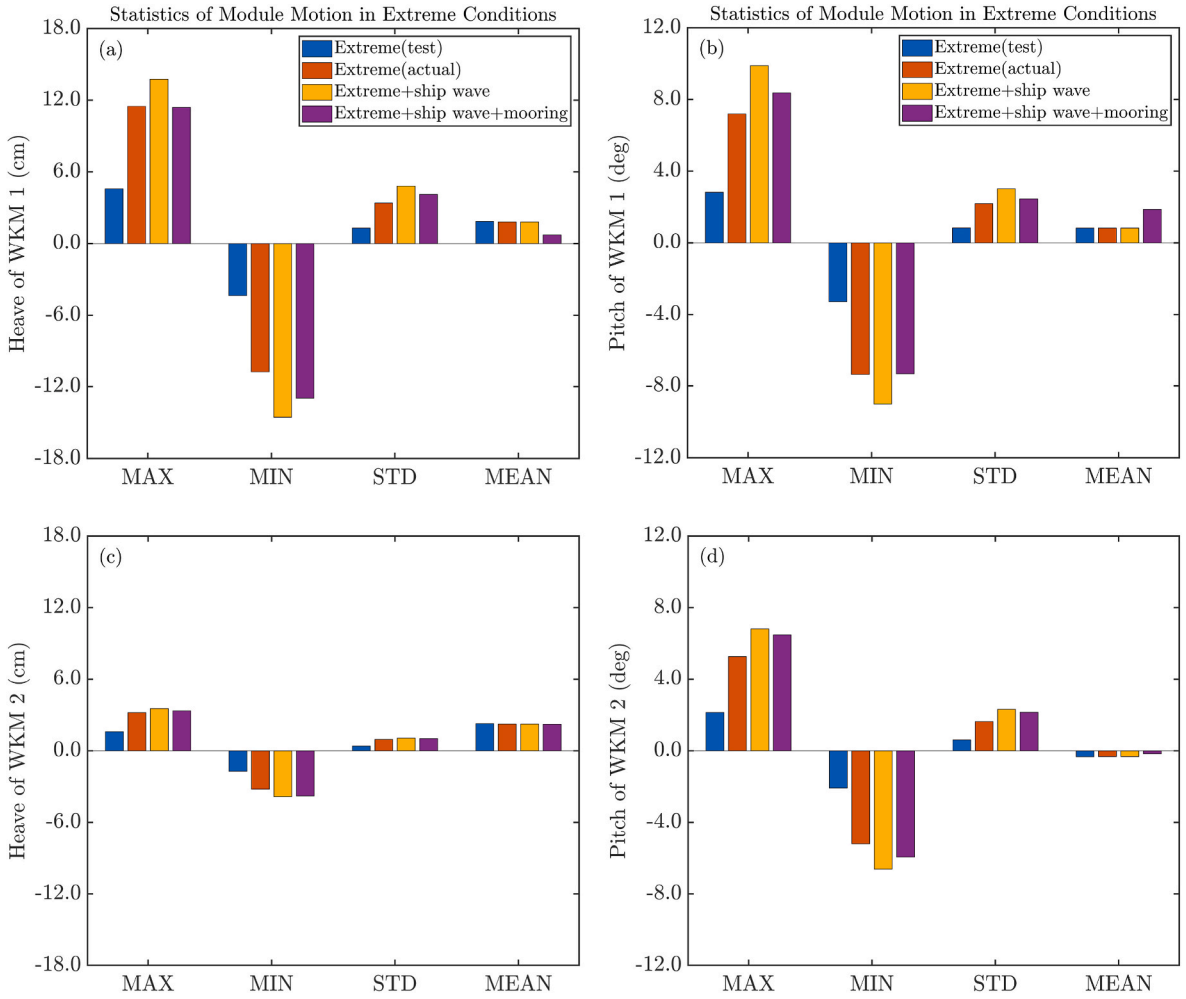

Fig. 18. Statistics of heave and pitch motions for walkway modules 1 (WKM 1) and 2 (WKM 2) in the extreme sea conditions.

The statistics of the motion responses of the two walkway modules, namely, WKM 1 and WKM 2, are shown in Fig. 18. It can be seen that when the significant wave height increases to 0.2 m, the maximum heave and pitch motions of the outermost walkway modules can reach 12 cm and 7°, respectively. If the ship wakes are considered, both responses will increase further by around 20 %. This indicates that the hydrodynamic effect induced by passing vessels for nearshore floating PV farms is important and should be considered in the design. By introducing the mooring lines, both the heave and pitch motions are reduced to a similar level as in the case where there are no ship wakes. This verifies that introducing mooring lines at the edges of the floating PV farm is beneficial for motion reduction of the farm. Besides, the responses of the walkway module WKM 2 are found to be dramatically smaller than WKM 1, indicating that the outermost modules need more attention in the design and operational phases.

Fig. 19 shows the corresponding connection forces at C4 and C6. The

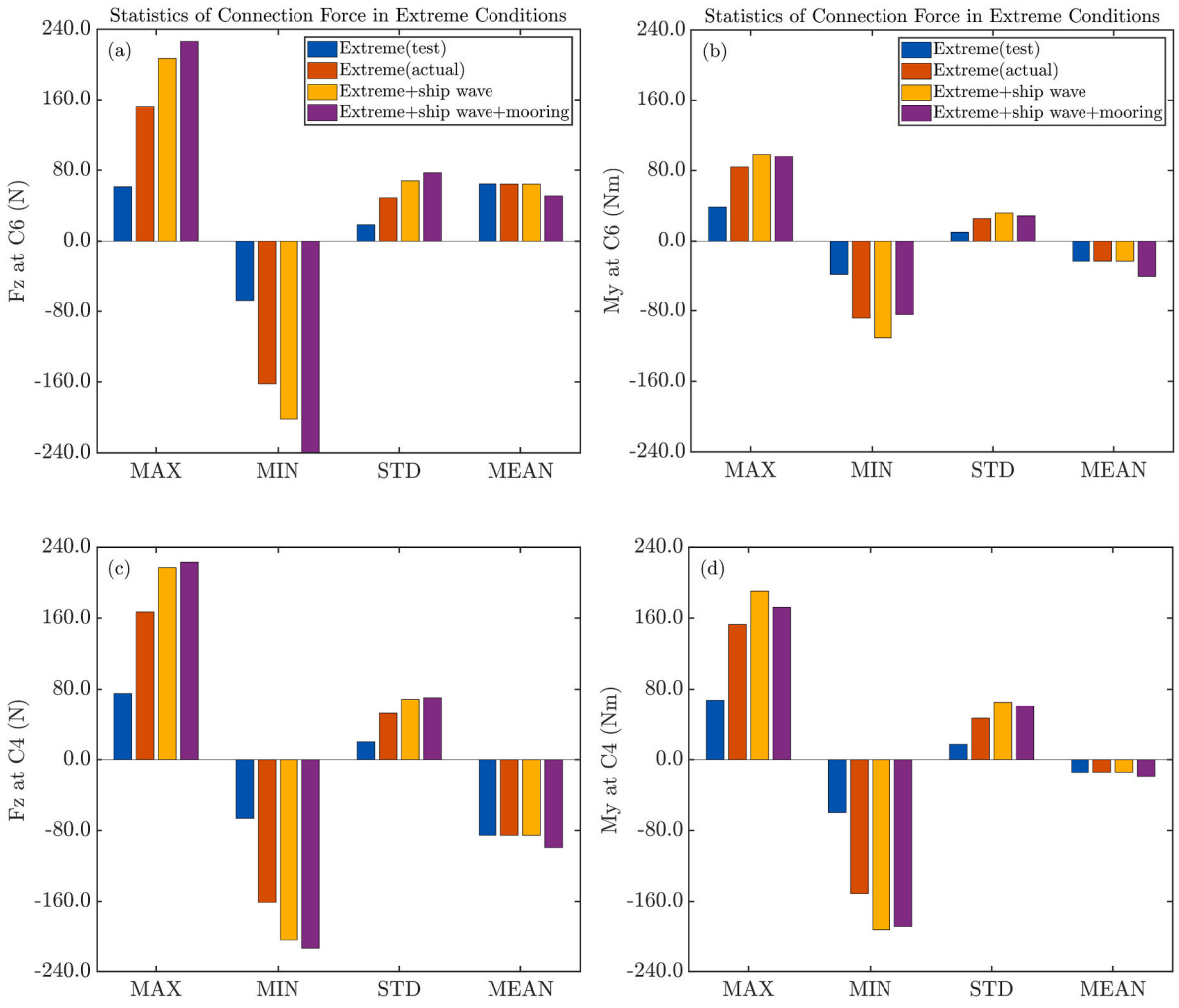

Fig. 19. Statistics of the force Fz and moment My at inter-module connection C4 and C6 in the extreme sea conditions.

locations of the two connections can be found in Fig. 14. With harsher sea conditions, the connection forces increase as expected. However, it is also found the connection forces Fz for both connections increase when mooring lines are introduced, contrary to the declining trend in the motion responses (see Fig. 18). It is also surprising to see the moment at connection C4 is almost doubled as compared to C6. The reduction in the motions has led to larger connection forces. These results indicate that a compromise between the motion and the connection forces has to be made in the design. Note that C4 is close to the pin constraints at the end of the subsystem with translation in the z-direction fixed. The boundary conditions imposed in the numerical model have led to larger Fz at C4. In the entire floating PV form, however, the connection forces are expected to be smaller.

7. Evaluation of operation and energy performance

The offshore floating PV farm located off Woodlands has been successfully operational since June 2021. Feedback from operators indicates excellent dynamic performance of the platform during its operation. To provide a more comprehensive evaluation of the farm's operational performance, an on-site monitoring system is planned. The system will capture various parameters, including drift motion, local responses, and connector forces. These parameters will be reported once they are available. Another crucial aspect of evaluation is the power generation performance of the PV farm. This evaluation is discussed in detail in this section.

Following the installation, site-testing and rectification of identified issues, the PV farm became fully operational in August 2021. Since then, the energy revenue data has been systematically monitored on an hourly, daily, and monthly basis. To better understand the power generation performance of the floating PV farm and the influencing factors, two sets of estimates are made. The results are then compared with the actual power generation reported at the site.

The first estimate is based on a simulation in PVWatts® calculator developed by National Renewable Energy Laboratory (NREL) and based on typical meteorological year (TMY) data. This is considered as the pre-installation calculation because the TMY data used for the simulations is up to the year of 2020, which is earlier than the installation of the PV farm. In the simulation, PVWatts® V8.1 is used, which introduced the updated weather data, namely Himawari TMY based solar resource data. More details on PVWatts and the methodology for the simulation can be found in Ref. [49].

The second estimate is made based on the historical meteorological data from the National Aeronautics and Space Administration (NASA) Langley Research Center (LaRC) Prediction of Worldwide Energy Resource (POWER) Project [38]. It is considered as the post-installation calculation since the historical solar irradiance data for the operational months of the PV farm are used.

The essential inputs for the power generation simulations include solar irradiance, system loss factor, and tilt and Azimuth angle. The TMY data for pre-installation calculation and the historical solar irradiance data from 2013 to 2022 are plotted in Fig. 20. As can be seen, significant variations in the monthly solar irradiance across different years are observed due to the changing weather conditions at the site. For both

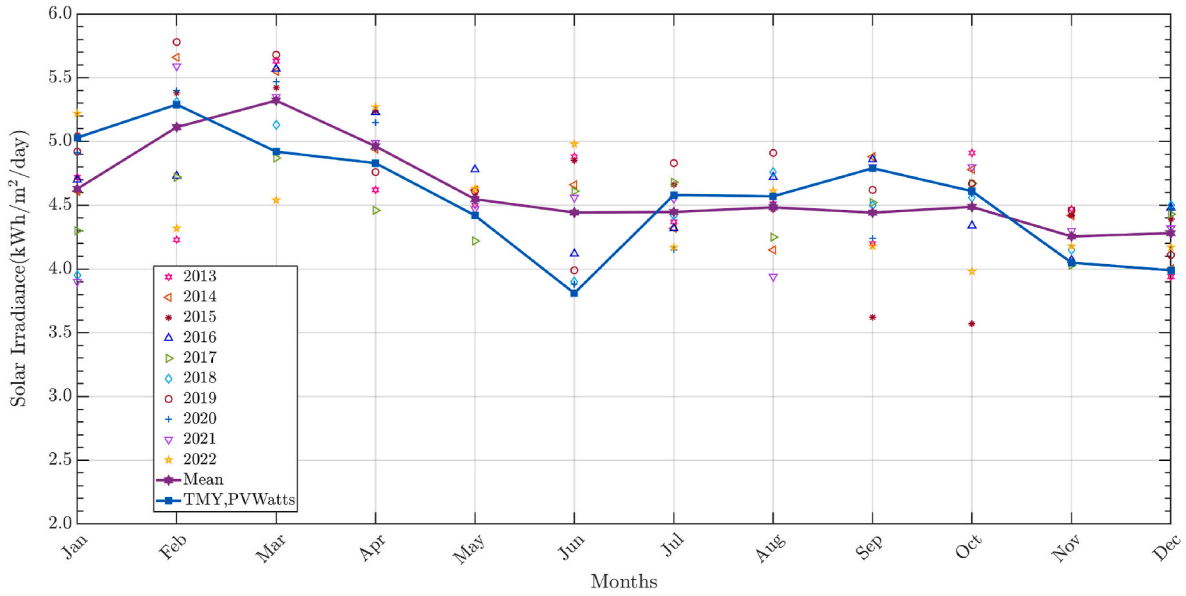

Fig. 20. Comparison of power generation between estimation and site monitoring.

calculations, a performance ratio of 80 % is applied. This ratio is selected by making a reference to the available site monitoring data corresponding to similar floating PV systems at the world's largest floating PV test bed which is close to the site [4] and the authors' previous work [33] conducted for a water reservoir condition in Singapore. The tilt angle of the PV panels is 10°. In reality, because of the wave-induced motion of the floating modules, the tilt angle might change dynamically. However, under the operational conditions, it has been proven from the hydrodynamic analysis and physical model tests presented in sections 4 and 5 that the wave-induced motions of the modules in the floating PV farm in this study are quite small and thus such an effect on the power generations is expected to be limited.

Then, the post-installation month power generation E can be calculated as

$$E = A \times r \times Q \times PR \tag{6}$$

where A is the total solar panel area in the floating PV system installation; r is the PV module efficiency ratio; Q is the solar radiation in a specific month; and PR is the performance ratio. Given that $A = 26000$ m^2, $r = 18.4$ % [50], Q taken from the daily average solar irradiance [38] as shown in Fig. 20 multiplied by the number of days in a specific month, and PR set to 80 % as already explained.

The results from the site and the estimates by using both the pre-installation and post-installation calculations are presented in Fig. 21, which lists the monthly energy revenue of the floating PV farm. Note that only the results from August 2021 to January 2022 are presented due to the availability of the site monitoring data. It can be found that the pre-installation calculations show some discrepancies (averagely 14.0 % difference) when compared to the site-monitoring data, while the post-installation calculations show much better agreement (averagely 2.0 % difference). This is induced by the variations in the TMY solar irradiance when compared to the historical data.

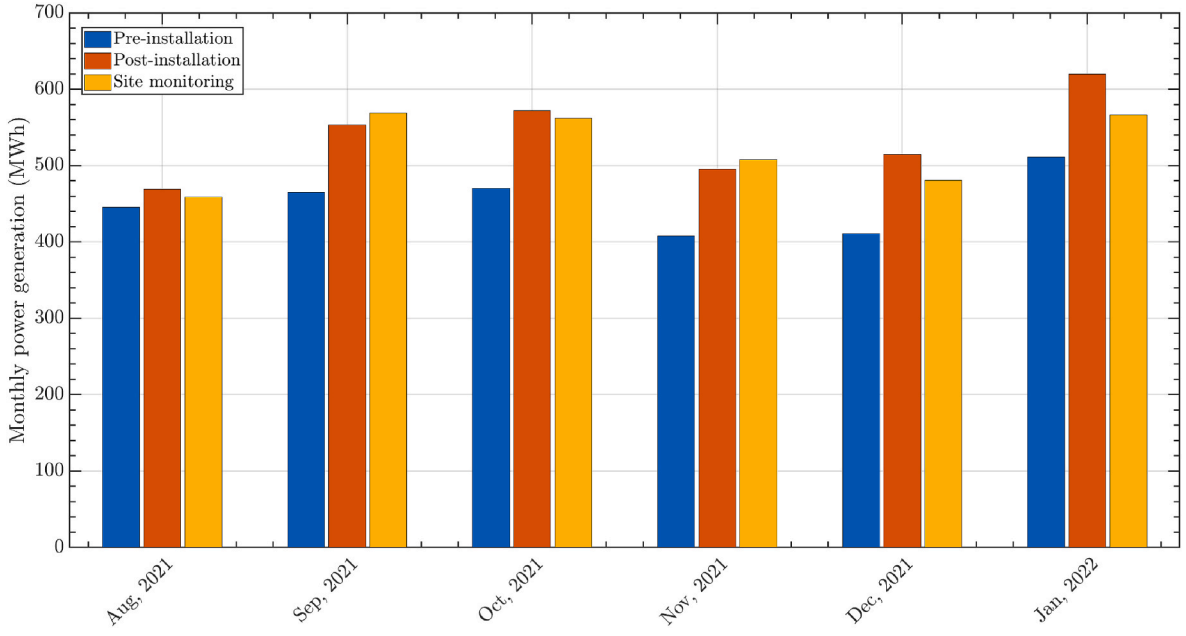

Fig. 21. Comparison of power generation between estimations and site monitoring data.

It is noted that the average monthly power generation has reached 524 MWh in these months. According to the Energy Market Authority of Singapore [51], the monthly national-average household electricity consumption is 272.4 kWh in 2021. The floating PV farm can support around 1875 households in Singapore, which is considered an important power generation source and contribution to achieving the national carbon neutralization goal.

The capacity factor (*CF*) of the floating PV farm is evaluated to understand the system capacity under actual environmental and PV farm availability conditions. The capacity factor is defined as the ratio of the actual power E_{actual} produced in a particular period of N days to the maximum possible power that can be produced by the system, namely,

$$CF = \frac{E_{actual}}{W_p \times 24 \times N} \tag{7}$$

where W_p is the system rated capacity.

The *CF* of this PV farm in real-world conditions over the period considered in this study is 15.2 %, which is in a reasonable range in the Southeast Asia region and Singapore [52], where the weather could be cloudy and rainy in the season. To further improve the performance, a tracking system may be introduced to boost the power generation on top of the presented floating PV farm system. This could be investigated in the future on the next-generation floating PV farms.

8. Uncertainty analysis

The entire design and verification framework integrates experimental tests, numerical simulations, and on-site monitoring, inherently introducing a blend of errors and uncertainties. These uncertainties include both random components (precision errors) and systematic components (bias errors). Quantifying these uncertainties necessitates a systematic analysis, which is challenging and sometimes even impossible. For example, assessing the precision error in model tests typically requires a large number of repetitions of the test cases, making it a resource-intensive endeavour.

In the uncertainty analysis, the focus is placed on identifying the primary sources of uncertainties within the verification analysis and qualitatively assessing their potential impact on the results of the study. The major uncertainties arise at three key steps of the study, namely, (1) characterization of environmental conditions and loads, (2) experimental and numerical studies, and (3) evaluation of the power generation performance.

In the characterization of environmental conditions and environmental loads, several sources of uncertainties arise and need to be carefully considered. First, the metocean data for the site location was provided by DHI. The nine years of wind data from the nearest meteorological station were investigated to develop ambient wind statistics and extreme. The design current conditions were derived solely based on simulated data obtained from DHI's hydrodynamic model, while the design incident wave conditions were based on wave hindcast data from DHI's spectral wave model. Both the hydrodynamic and spectral wave models for the site location were not calibrated in the absence of available field survey. However, DHI hosts a database of numerical models that can broadly be described as pre-validated on a regional scale, which limits the uncertainty of the characterized environmental conditions. Second, wind loads were not accounted for in the verification analysis as the focus was placed on the global responses of the floating PV farm. The wind loads are expected to have limited influence on the global motion, considering the rather low elevation of the farm above the sea level. However, the effect of wind loads was considered in the analysis and design of the connection between PV panels and floating modules. Third, the use of an empirical model for estimating the ship wakes may also introduce a certain degree of uncertainty due to the variation of vessel types in this region. Finally, from the long-term operational perspective, the effects due to climate change, such as sea level rise and worse sea conditions may occur and affect the operational performance of the floating PV farm. Such effects are not considered in the characterization of the design environmental conditions over the design life span of the farm. To address these uncertainties, one may install on-site monitoring systems which can be used to support a risk-based analysis and predictions of the status of the farm.

In the experimental study, sources of uncertainties are mainly from wave generations, model setup, and instrumentation and measurement. The generated waves were calibrated before the basin test, which revealed a 5 % difference in the significant wave heights and peak periods between the targeted and generated wave spectra. Uncertainties were also identified in the model setup, including a 2–3% difference in the mass distributions between the prototype and the model, less than 10 % wave reflections from the basin walls, and frictions in the boundary which was not possible to quantify. The instrumentations were all calibrated before the basin test, and the reported errors for translational motions are within $\pm$ 1 mm and rotational motions are within $\pm$ 0.1°. The uncertainty in the numerical simulations is mainly from the neglection of nonlinearity in the mooring system and fluid viscous effects. In general, these uncertainties are considered as not significant in view of the fact that the results generated by the numerical model agree well with the experimental data.

In the evaluation of the power generation performance, uncertainties may be introduced through the accuracy of the site monitoring devices, e.g., sampling rate and system calibrations. Besides, the maintenance schedule of the floating PV farm and the monitoring devices were not considered in the study. In addition, there is a lack of actual solar irradiance data at the site location. Furthermore, the effect of wave-induced motion of the floating modules on the power generation of PV panels was not investigated. A long-term physical monitoring campaign will provide valuable results for quantifying the uncertainties in the power generation performance of the floating PV farm.

9. Conclusion

In this study, the design and verification methodologies for a floating PV farm in coastal marine conditions are presented through a practical example of the recently deployed world's largest 5 MW nearshore floating PV farm in the coastal region of Singapore. The aim is to present a framework with practical methodologies involving essential design considerations, design verification methods and real-world power generation evaluation for coastal floating PV farm development.

The design considerations of the 5 MW coastal floating PV farm were presented. These include marine biofouling, special design for the mooring system, special design to enhance the reliability of the inter-module connectors as well as the consideration of special coastal environmental conditions, in particular ship wakes. Details on the considerations of these factors were demonstrated on the 5 MW nearshore floating PV farm. These design considerations, drawn from the practical deployment, are pivotal for addressing the unique challenges of coastal marine conditions and was rarely reported in the literature.

The method for verification of the floating PV farm in coastal marine conditions focused on a small-scale subsystem of the entire large floating system. Laboratory tests and numerical simulations were conducted. Through the laboratory experiments and the corresponding numerical simulations, it was found that the hydrodynamic performance of the subsystem of the pontoon-type floating PV farm in the nearshore region is excellent. Based on the validated multibody numerical models, the effect of ship wakes on floating PV farms is considered and investigated for the first time. It is found that the waves generated by passing ships can induce significant motions of the PV farms. Proper protection of the PV farms may be necessary when it is constructed beside a busy waterway. The study also investigated the effect of mooring lines, which shows that introducing mooring lines can reduce the motion of the outermost modules. However, it cannot reduce the connection forces. It is important to make a strengthened design for the modules in those

regions and conduct frequent checks during regular maintenance.

The final critical step involves comprehensive on-site monitoring, encompassing both the dynamic responses of the floating PV farm and the performance of power generation. Although a plan for on-site monitoring of structural responses for the 5 MW floating solar farm off Woodlands has been formulated, it has yet to be implemented. However, an assessment of power generation performance was conducted after the platform was connected to the grid. The results are highly promising, revealing a monthly average power generation exceeding 500 MWh, which could support 1875 households in Singapore and contribute to expedite the decarbonization process. The capacity factor of the farm is around 15.2 % which is within a reasonable range in Singapore and Southeast Asia.

The design considerations outlined for the practical development of one of the world's largest commercial floating PV farms in coastal marine conditions, along with the methodologies for verifying its performance, are expected to serve as valuable references for future floating PV farm developments in nearshore waters. Subsequent research efforts will prioritize the validation of floating PV farm designs through real-world data collection by implementing on-site monitoring systems. Although the case study is based on Singaporean environmental conditions, the methodologies presented can be applied to the design and verification of floating PV farms or similar structures elsewhere with appropriate modifications and considerations of the site-specific conditions. In environmentally exposed locations, wind and wave loads may induce substantial motions of the floating modules, which may affect the power generation performance of the PV panels. Besides, sun-tracking systems and different energy systems to improve the power generation performance of floating PV farms are worth further investigating.

CRediT authorship contribution statement

Chi Zhang: Conceptualization, Methodology, Formal analysis, Writing – original draft, Visualization. **Jian Dai:** Conceptualization, Methodology, Formal analysis, Writing – review & editing, Visualization. **Kok Keng Ang:** Conceptualization, Resources, Writing – review & editing. **Han Vincent Lim:** Resources, Project administration.

Declaration of competing interest

The authors declare the following financial interests/personal relationships which may be considered as potential competing interests: Jian Dai reports equipment, drugs, or supplies was provided by Sunseap Group. Jian Dai reports administrative support was provided by Singapore Housing and Development Board. Jian Dai reports equipment, drugs, or supplies was provided by G8 SUBSEA.

Data availability

Data will be made available on request.

Acknowledgment

The authors gratefully acknowledge Sunseap Group, Housing & Development Board of Singapore and G8 SUBSEA for providing the data and information. Any opinions, findings, and conclusions or recommendations expressed in this study are those of the authors and do not reflect the views of Sunseap Group, Housing & Development Board of Singapore and G8 SUBSEA.

References

[1] International Energy Agency. Global energy review 2021. Paris: International Energy Agency; 2021.
[2] Luther J, Reindl T, Wang DKS, Aberle A, Walsh W, Nobre A, Yao GG. Solar photovoltaic (PV) roadmap for Singapore (A summary). Singapore: Solar Energy Research Institute of Singapore (SERIS); 2013.
[3] Reindl T, Kong X, Pathare A. Update of the solar photovoltaic (PV) roadmap for Singapore. Singapore: Solar Energy Research Institute of Singapore (SERIS); 2020.
[4] Liu H, Krishna V, Lun Leung J, Reindl T, Zhao L. Field experience and performance analysis of floating PV technologies in the tropics. Prog Photovoltaics Res Appl 2018;26(12):957–67.
[5] Vidović V, Krajačić G, Matak N, Stunjek G, Mimica M. Review of the potentials for implementation of floating solar panels on lakes and water reservoirs. Renew Sustain Energy Rev 2023;178:113237.
[6] Kim SH, Yoon SJ, Choi W, Choi KB. Application of floating photovoltaic energy generation systems in South Korea. Sustainability 2016;8(12):1333.
[7] Mursid O, Malau KR, Huda N, Abidin AMA, Sutarno G. Design and feasibility studies a floating photovoltaic to supply electricity for isolated island village in Indonesia. In: IOP conference series: earth and environmental science, vol. 698. IOP Publishing; 2021, 012033. 1.
[8] Tina GM, Rosa-Clot M, Rosa-Clot P, Scandura PF. Optical and thermal behavior of submerged photovoltaic solar panel: SP2. Energy 2012;39(1):17–26.
[9] Choi YK. A study on power generation analysis of floating PV system considering environmental impact. Int J Softw Eng its Appl 2014;8(1):75–84.
[10] El Hammoumi A, Chalh A, Allouhi A, Motahhir S, El Ghzizal A, Derouich A. Design and construction of a test bench to investigate the potential of floating PV systems. J Clean Prod 2021;278:123917.
[11] Dörenkämper M, Wahed A, Kumar A, de Jong M, Kroon J, Reindl T. The cooling effect of floating PV in two different climate zones: a comparison of field test data from The Netherlands and Singapore. Sol Energy 2021;219:15–23.
[12] Pouran HM, Lopes MPC, Nogueira T, Branco DAC, Sheng Y. Environmental and technical impacts of floating photovoltaic plants as an emerging clean energy technology. iScience 2022;25(11):105253.
[13] Yang P, Chua LH, Irvine KN, Nguyen MT, Low EW. Impacts of a floating photovoltaic system on temperature and water quality in a shallow tropical reservoir. Limnology 2022;23(3):441–54.
[14] Exley G, Page T, Thackeray SJ, Folkard AM, Couture RM, Hernandez RR, Armstrong A. Floating solar panels on reservoirs impact phytoplankton populations: a modelling experiment. J Environ Manag 2022;324:116410.
[15] Eisl R, Haider M. Heliofloat – a floating lightweight platform. 2016. https://www.tuwien.at/fileadmin/Assets/dienstleister/forschungsmarketing/messe/Messe_Rueckblick/HM2016/HELIOFLOAT_platform_EN.pdf. [Accessed 14 January 2022].
[16] Putschek M. Experiences of marine floating PV projects. In: Intersolar conference 2018; 2018. Munich, Germany.
[17] DNV KEMA. SUNdy, a floating solar field concept. Technical Report Document. Utrechtseweg: DNV KEMA; 2018.
[18] Jiang Z, Dai J, Saettone S, Tørå G, He Z, Bashir M, Souto-Iglesias A. Design and model test of a soft-connected lattice-structured floating solar photovoltaic concept for harsh offshore conditions. Mar Struct 2023;90:103426.
[19] Sahu A, Yadav N, Sudhakar K. Floating photovoltaic power plant: a review. Renew Sustain Energy Rev 2016;66:815–24.
[20] Zhang C, Santo H, Magee AR. Review and comparative study of methodologies for hydrodynamic analysis of nearshore floating PV farms. In: Offshore technology conference Asia. OnePetro; 2022.
[21] Claus R, López M. Key issues in the design of floating photovoltaic structures for the marine environment. Renew Sustain Energy Rev 2022;164:112502.
[22] Zhang C. Hydrodynamics of large compliant modular floating structures, Doctoral Thesis. Singapore: National University of Singapore; 2020.
[23] Zhang C, Wan L, Magee AR, Han M, Jin J, Ang KK, Hellan Ø. Experimental and numerical study on the hydrodynamic loads on a single floating hydrocarbon storage tank and its dynamic responses. Ocean Eng 2019;183:437–52.
[24] Ren N, Zhang C, Magee AR, Hellan Ø, Dai J, Ang KK. Hydrodynamic analysis of a modular multi-purpose floating structure system with different outermost connector types. Ocean Eng 2019;176:158–68.
[25] Karpouzoglou T, Vlaswinkel B, van der Molen J. Effects of large-scale floating (solar photovoltaic) platforms on hydrodynamics and primary production in a coastal sea from a water column model. Ocean Sci 2020;16(1):195–208.
[26] Kriebel DL, Seelig WN, Judge C. Development of a unified description of ship-generated waves. In: Proceedings of the U.S. Section PIANC annual meeting, roundtable, and technical workshops (CD-ROM). Alexandria, VA, USA: PIANC USA; 2003.
[27] Det Norske Veritas. Recommended practice DNVGL-RP-0584: design, development, and operation of floating solar photovoltaic systems. Oslo: Det Norske Veritas; 2021.
[28] Xu P, Wellens PR. Fully nonlinear hydroelastic modeling and analytic solution of large-scale floating photovoltaics in waves. J Fluid Struct 2022;109:103446.
[29] Wei Y, Ou B, Wang J, Yang L, Luo Z, Jain S, et al. Simulation of a floating solar farm in waves with a novel sun-tracking system. In: IOP conference series: materials science and engineering, vol. 1288. IOP Publishing; 2023, 012041. 1.
[30] Ikhennicheu M, Danglade B, Pascal R, Arramounet V, Trébaol Q, Gorintin F. Analytical method for loads determination on floating solar farms in three typical environments. Sol Energy 2021;219:34–41.
[31] Faltinsen O. Sea loads on ships and offshore structures. Cambridge University Press; 1993.
[32] Al-Yacouby AM, Halim ERBA, Liew MS. Hydrodynamic analysis of floating offshore PV farms subjected to regular waves. In: Advances in manufacturing engineering. Singapore: Springer; 2020. p. 375–90.
[33] Claus R, López M. A methodology to assess the dynamic response and the structural performance of floating photovoltaic systems. Sol Energy 2023;262:111826.
[34] Dai J, Zhang C, Lim HV, Ang KK, Qian X, Wong JLH, et al. Design and construction of floating modular photovoltaic system for water reservoirs. Energy 2020;191:116549.

[35] Sree DK, Law AWK, Pang DSC, Tan ST, Wang CL, Kew JH, et al. Fluid-structural analysis of modular floating solar farms under wave motion. Sol Energy 2022;233:161–81.
[36] Delacroix S, Bourdier S, Soulard T, Elzaabalawy H, Vasilenko P. Experimental modelling of a floating solar power plant array under wave forcing. Energies 2023;16(13):5198.
[37] Borvik PP. Experimental and numerical investigation of floating solar islands, Master's Thesis. Trondheim: Norwegian University of Science and Technology; 2017.
[38] National Aeronautics and Space Administration (NASA). Prediction of worldwide energy resource (POWER) project. 2023. https://power.larc.nasa.gov. [Accessed 10 September 2023].
[39] Danish Hydraulic Institute. Woodlands data provision. May 2018. Technical Report No. 61802197.
[40] Gharbi S, Valkov G, Hamdi S, Nistor I. Numerical and field study of ship-induced waves along the St. Lawrence Waterway, Canada. Nat Hazards 2010;54(3):605–21.
[41] David CG, Roeber V, Goseberg N, Schlurmann T. Generation and propagation of ship-borne waves-Solutions from a Boussinesq-type model. Coast Eng 2017;127:170–87.
[42] Kriebel DL, Seelig WN. An empirical model for ship-generated waves. In: Proceedings of the Fifth International Symposium on Ocean Wave Measurement and Analysis; 2005. Madrid.
[43] Larson M, Almström B, Göransson G, Hanson H, Danielsson P. Sediment movement induced by ship-generated waves in restricted waterways. Coast Dyn 2017;120:300–11.
[44] Zhang C, Fonseca N, Ren N, Magee AR, Ang KK. Experimental and numerical investigation of wave-induced hydrodynamic interactions of a sub-floating hydrocarbon storage tank system in shallow waters. Ocean Eng 2020;216:108104.
[45] Cummins WE, Iiuhl W, Uinm A. The impulse response function and ship motions. David Taylor Model Basin–DTNSRDC; 1962. Technical Report 1661.
[46] Lee C, Newman JN. WAMIT v7.3 user manual. WAMIT Inc; 2019.
[47] Babarit A, Gérard D. Theoretical and numerical aspects of the open source BEM solver NEMOH. In: 11th European wave and tidal energy conference (EWTEC2015); 2015.
[48] Yu Y-H, Lawson M, Ruehl K, Michelen C. Development and demonstration of the WEC-Sim wave energy converter simulation tool. In: Proceedings of the 2nd marine energy technology symposium. Seattle, WA: METS 2014; 2014.
[49] Dobos AP. PVWatts version 5 manual (No. NREL/TP-6A20-62641). Golden, CO (United States): National Renewable Energy Lab. (NREL); 2014.
[50] Eagle JinkoSolar. Dual 72 350-370 Watt monocrystalline module manual. JinkoSolar; 2018.
[51] Energy Market Authority. Energy consumption chapter 03. https://www.ema.gov.sg/singapore-energy-statistics/Ch03/index3. [Accessed 9 May 2022].
[52] International Renewable Energy Agency and ASEAN Center for Energy. Renewable energy outlook for ASEAN: towards a regional energy transition. second ed. 2022. https://www.irena.org/publications/2022/Sep/Renewable-Energy-Outlook-for-ASEAN-2nd-edition. [Accessed 16 September 2023].